RSC Advances

ROYAL SOCIETY OF CHEMISTRY

www.rsc.org/advances

Journal Name

ARTICLE

2,4-Bis(4-aryl-1,2,3-triazol-1-yl)pyrrolo[2,3-*d*]pyrimidines: Synthesis and Tuning of Optical Properties by Polar Substituents

Received 00th January 20xx,
Accepted 00th January 20xx

DOI: 10.1039/x0xx00000x

www.rsc.org/

Jonas Bucevicius,[a] Lina Skardziute,[b] Jelena Dodonova,[a] Karolis Kazlauskas,[b] Gintautas Bagdziunas,[c] Saulius Jursenas,[b] Sigitas Tumkevicius*[a]

2,4-Bis(4-aryl-1,2,3-triazol-1-yl)pyrrolo[2,3-*d*]pyrimidines as D-π-A-π-D chromophores were successfully prepared by CuAAC reaction of 2,4-diazido-7-methylpyrrolo[2,3-*d*]pyrimidine with ethynylarenes in dichloromethane in the presence of CuI/DIPEA/AcOH as a catalyst system. The incorporation of small polar substituents enabled tuning of the energy of frontier orbitals and thus, the FMOs energy gap by up to 0.9 eV, while the incorporation of bulky steric substituents resulted in narrowing of the energy gap by up to 0.4 eV. Owing to electron-accepting properties of pyrrolo[2,3-*d*]pyrimidine core extending to triazole moieties the compounds with electron-donating groups showed expressed intramolecular charge transfer character (ICT) of the excited states which was proved by solvatochromic dynamics and supported by DFT calculations. The optimization of ICT reduced radiative and non-radiative deactivation pathways resulted in enhancement of fluorescence quantum yield up to 73%.

Introduction

Over recent years, organic molecules with a π-conjugated backbone have received much attention in both academic and industry due to their applications in a wide range of electronic and optoelectronic devices.[1] Introduction of heteroaryl moieties into the backbone of extended π-systems considerably influences molecular orbitals, stereochemical structure and linking topology of the substituents. In this regard, pyrimidine ring containing heterocycles owing to their aromaticity, significant π-deficiency, and ability of nitrogen atoms to take part in the chelation processes, are desired structural units to be incorporated in more complex organic structures targeted for numerous applications.[2] Pyrimidine moiety has already been incorporated into linear, star- and banana-shaped oligomers that show good light emitting properties and two-photon absorption.[3] Moreover, pyrimidine ring is frequently used in push-pull structures as strong electron-withdrawing unit and together with electron-donating moieties results in intramolecular charge transfer character, which plays a key role in most of the important applications.[3a, 3d, 3e, 3g-h] Particularly, the applications of intramolecular charge transfer complexes has recently attracted attention due to invention of delayed fluorescence emitters, possessing nitrogen heterocycles.[4] Another important use of donor-acceptor structures is fluorescence bio-material labelling and metal ions sensing.[5] Generally, these push-pull chromophores have an A-π-D structure, where A is an electron-withdrawing moiety and D is an electron-donating group connected by a π-conjugated linker. Since the discovery of Cu(I)-catalyzed Huisgen azide-alkyne cycloaddition (CuAAC) by Sharpless[6] and Meldal[7] many examples that incorporate the 1,2,3-triazole moiety have been reported. CuAAC provides 1,4-disubstituted 1,2,3-triazoles with such efficiency and scope that transformation is usually referred as "click" chemistry and is one of the most atom-economical transformations.[8] Various 1,2,3-triazoles have found application in fields of bioconjugation,[9] material science,[10] chemical sensors[11] and drug discovery.[12] More recently, the 1,2,3-triazole unit as a linker in the conjugated backbone of fluorescent and two-photon absorption compounds has been investigated.[3e, 3f, 13] Structure-photophysical properties relationships of some push-triazole-pull chromophores revealed the 1,2,3-triazole is better π-conjugated linker in terms of both, quantum yields and Stokes shifts than the triple bond.[3e, 3f] Recently, we have shown that pyrrolo[2,3-*d*]pyrimidines bearing π-conjugated aromatic assemblies as side branches exhibit strong UV-blue fluorescence and are promising candidates as fluorescent functional materials.[14] Continuing our work aimed to the search of novel fluorescent materials we became interested in the synthesis of pyrrolo[2,3-*d*]pyrimidine derivatives with a 1,2,3-triazole linker between the aromatic side chains and heterocyclic scaffold. In the current literature triazolylpyrrolo[2,3-*d*]pyrimidines have received very little attention. To the best of our knowledge, there are only few

[a] Vilnius University, Department of Organic Chemistry, Naugarduko 24, LT-03225 Vilnius, Lithuania.
[b,b] Institute of Applied Research, Vilnius University, Sauletekio 9-III, LT-10222 Vilnius, Lithuania.
[c] Kaunas University of Technology, Department of Polymer Chemistry and Technology, Radvilenu 19, LT-50254 Kaunas, Lithuania.
Electronic Supplementary Information (ESI) available: [details of any supplementary information available should be included here]. See DOI: 10.1039/x0xx00000x

reports on the synthesis of pyrrolo[2,3-*d*]pyrimidines containing 1,2,3-triazole moiety. Using azide-alkyne ligation reaction 1,2,3-triazole moiety was constructed at the C5 or N7 position of the pyrrolopyrimidine ring[12b, 15] and none of these reactions were carried out using azidopyrrolo[2,3-*d*]pyrimidines as reactive partners.

The aim of this work is to describe the synthesis of new D-π-A-π-D chromophores that contain pyrrolo[2,3-*d*]pyrimidine system as electron-attracting part and substituted aromatic moieties as the electron-donating parts. The central pyrrolo[2,3-*d*]pyrimidine core and the external aromatic parts are linked by the π–conjugated electron accepting 1,2,3-triazole rings. The impact of the polar and steric substituents on the photophysical properties of the synthesized D-π-A-π-D chromophores were assessed by thorough analysis of their optical and electrochemical properties in various surroundings and the results of DFT modelling. Substituent induced altering of the excited state recombination pathways is discussed with special emphasis on the enhancement of fluorescence efficiency.

Results and discussion

Synthesis

The starting material - 2,4-diazido-7-methylpyrrolo[2,3-*d*]pyrimidine (**2**) was obtained in 78% yield by nucleophilic substitution of 2,4-dichloro-7-methylpyrrolo[2,3-*d*]pyrimidine (**1**) with NaN_3 in DMF at ambient temperature (Scheme 1). It should be mentioned that diazide **2** is rather unstable in daylight and at elevated temperatures, but can be stored for a long period of time in the dark below 5 °C. Azides of nitrogen heterocycles bearing azido group in an adjacent position to an endocyclic nitrogen atom can undergo spontaneous cyclization to form a tetrazole ring. The azide-tetrazole equilibrium is often observed in π-deficient heterocycles such as azidopyrimidines[16] and azidopurines.[9g, 17] Earlier reports on the synthesis of 4-azidopyrrolo[2,3-*d*]pyrimidines[18] indicate that these compounds in a solid state exist as a tetrazole tautomer. However, in the IR spectrum of compound **2** two absorbtion bands of both azido groups at 2152 cm^{-1} and 2115 cm^{-1} in KBr, and 2147 cm^{-1} and 2132 cm^{-1} in $CHCl_3$ are observed. ^1H NMR spectrum of compound **2** recorded in $CDCl_3$ indicated that compound **2** exists mainly in one tautomeric form in the solution. A ratio of diazide and another possible tetrazole tautomer was found to be 99:1, respectively. These data suggest that in a solid state and in the chloroform solution diazido form of compound **2** predominates.

Further, on the example of reaction of diazide **2** with 3-ethynyltoluene formation of 2,4-bis(triazolyl)pyrrolo[2,3-*d*]pyrimidine was investigated (Table 1). It was found that no ligation of diazide **2** with 3-ethynyltoluene occurred using well established $CuSO_4$/Na ascorbate catalyst system at ambient temperature in *t*-BuOH/H_2O (Table 1, entry 1). The target compound **3a** was obtained in 18% yield only when the reaction temperature was raised up to 70 °C (Table 1, entry 2). Low yield, probably, arises from low stability of diazide **2** at elevated temperatures. Another popular catalyst system CuI/NEt_3 was examined in different solvents. Cycloaddition reaction did not occur in DMF, DMSO and THF at room temperature (Table 1, entries 3, 4, 5). However, in dichloromethane CuAAC reaction took place to give a mixture of two regioisomers **3a** and possibly, **4a** in overall 30% yield with a ratio 71:29 as determined from ^1H NMR spectra (Table 1, entry 6). Addition of acetic acid, which is known to accelerate protonation of C-Cu bond,[19] raised the overall yield up to 48% (Table 1, entry 7). Switching base from TEA to DIPEA afforded a mixture of **3a** and **4a** in overall 78% yield (Table 1, entry 8). In all cases stated above regioisomeric ratio in the cycloaddition reaction of **2** with 3-ethynyltoluene was almost the same, so regioselectivity of this reaction seems to be not affected by the reaction conditions. To our knowledge, there are only few reports on the formation of 1,5-isomers in CuAAC reaction.[17, 20] 1,5-Disubstituted 1,2,3-triazoles as by-products can be formed by a competitive non-catalyzed thermal Huisgen cycloaddition, therefore, experiments were conducted in the absence of copper source and additives. However, no traces of the reaction products were observed even after 7 days (Table 2, entries 9, 10). This indicates that both isomers are formed by CuAAC pathway. Perhaps, presence of copper catalyst lowers activation energy barriers of the formation of both, 1,4- and 1,5-disubstituted isomers.[21]

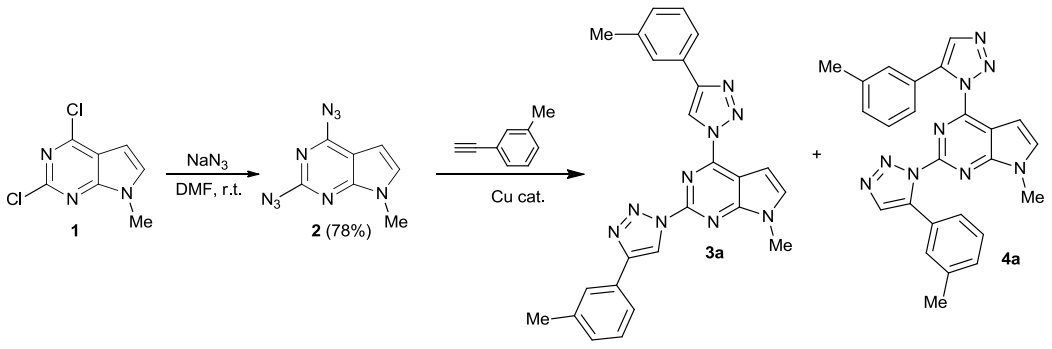

Scheme 1. Synthesis of 2,4-diazido-7-methylpyrrolo[2,3-*d*]pyrimidine (**2**) and model CuAAC reaction of with 3-ethynyltoluene.

Table 1. Optimization of CuAAC reaction of 2,4-diazido-7-methylpyrrolo[2,3-*d*]pyrimidine (**2**) with 3-ethynyltoluene.

Entry	Copper source/additive[a]	Solvent	Temp. (°C), time (h)	**3a**:**4a**[b]	Overall yield, % (**3a** + **4a**)
1	$CuSO_4$/Na ascorbate	*t*-BuOH/H_2O 2:1	rt, 72h	-	no reaction
2	$CuSO_4$/Na ascorbate	*t*-BuOH/H_2O 2:1	70, 48h	-	18[c]
3	CuI/NEt_3	DMSO	rt, 48h	-	decomposition products of **2**
4	CuI/NEt_3	DMF	rt, 48h	-	decomposition products of **2**
5	CuI/NEt_3	THF	rt, 96h	-	trace
6	CuI/NEt_3	CH_2Cl_2	rt, 96h	71:29	30
7	CuI/NEt_3/AcOH	CH_2Cl_2	rt, 72h	73:27	48
8	CuI/DIPEA/AcOH	CH_2Cl_2	rt, 72h	70:30	78
9	-	CH_2Cl_2	rt, 168h	-	no reaction
10	DIPEA/AcOH	CH_2Cl_2	rt, 168h	-	no reaction

[a] Reaction conditions: azide **2** (0.46 mmol), alkyne (1.4 mmol), copper source (20 mol%), trialkylamine (0.51 mmol), AcOH (0.51mmol), solvent (5 mL). [b] ^{1}H NMR ratio of the crude product. [c] Yield of 1,4-isomer **3a.**

Theoretically, the cycloaddition reaction of diazide **2** with alkynes can lead to the formation of four isomeric triazoles. The regiochemistries of the formed 2,4-bis(triazolyl)pyrrolo[2,3-*d*]pyrimidines were assigned on the basis of the characteristic ^{1}H NMR chemical shifts for positions C4-H and C5-H of the triazole moieties. Here, structural assignment of the formed regioisomers is illustrated on the example of compound **3d**, because none of the 5-H/4-H peaks of 1,2,3-triazole in ^{1}H NMR spectra of its isomeric mixture were overlapped. For clarity, in Figure 1 structures of all possible isomers of 4-(dimethylamino)phenyl derivative **3d-6d** are presented. It is known that 5-H signal in the ^{1}H NMR spectra of 1,4-disubstituted-1,2,3-triazoles is usually observed in lower fields than 4-H peak of 1,5-disubstituted-1,2,3-triazoles.[13d, 17, 22]

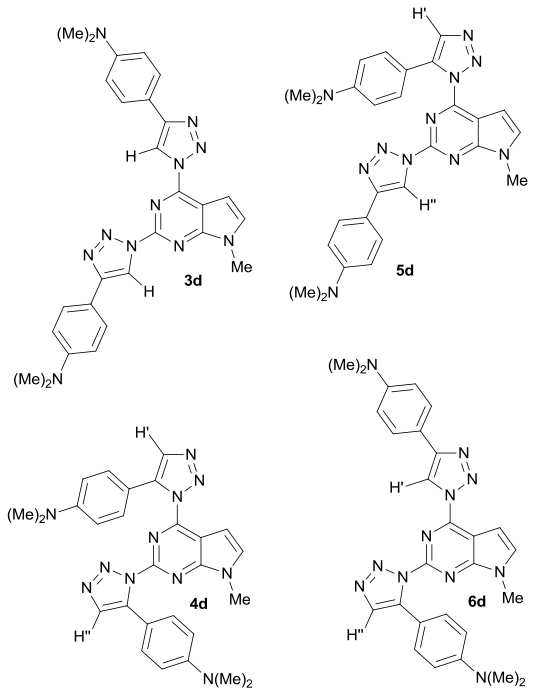

Figure 1. Structures of possible isomers 3d-6d of ligation reaction of 2 with 4-(dimethylamino)phenylethyne.

Analogous relationship was observed in the ^{1}H NMR spectra of compounds **3** and **4**. For example, in the ^{1}H NMR spectrum of a mixture of **3d** and **4d** both 5-H peaks of isomer **3d** are observed at 8.93 ppm and 8.72 ppm, while the 4-H peaks of **4d** are located at 7.80 ppm and 7.52 ppm, respectively (Table 2). It is logical to assume that in case of any "mixed" isomer (**5d** or **6d**) only one of the peaks would be shifted to higher fields. In addition, geometries of all regioisomers **3d**-**6d** were optimized by DFT/B3LYP/6-311G** level of theory and shielding values of the corresponding 4-H and 5-H of 1,2,3-triazole moieties were computed by GIAO method. Comparison of the calculated chemical shifts of 4-H and 5-H of the triazole rings for compounds **3d**-**6d** with the experimental values (Table 2) also indicates that in the reaction of diazide **2** with 4-(dimethylamino)phenylethyne the corresponding 1,4-disubstituted (**3d**) and 1,5-disubstituted 1,2,3-triazoles (**4d**) were formed.

Table 2. Calculated and experimental chemical shifts of 1,2,3-triazole 4H and 5H protons for possible isomers **3d**-**6d**.

	Calculated shifts, δ, ppm				Experimental shifts, δ, ppm	
	3d	**4d**	**5d**	**6d**	**3d**	**4d**
H'	9.28	7.73	7.66	9.15	8.93	7.80
H''	8.98	7.53	8.90	7.69	8.72	7.52

Having established that the optimal CuAAC reaction conditions were CuI/DIPEA/AcOH/CH_2Cl_2 we next turned our attention to the scope of the cycloaddition of diazide **2** with a range of arylethynes. In most cases, alkynes underwent ligation with diazide **2** to give mixtures of bis-triazoles **3** and **4** with overall yields varying from 62% to 89% (Table 3). Cycloaddition of **2** proceeds faster with arylethynes bearing electron-withdrawing substituents (Table 3, entries 5-7). Regioselectivity favors the formation of 1,4-isomer. The lowest regioselectivity (63:37) and the lowest yield of 1,4-isomer was obtained when 4-(dimetylamino)phenylethyne bearing strong electron donating group was employed in the reaction (Table 3, entry 4).

Table 3. Synthesis of bistriazoles **3a-l** by CuAAC

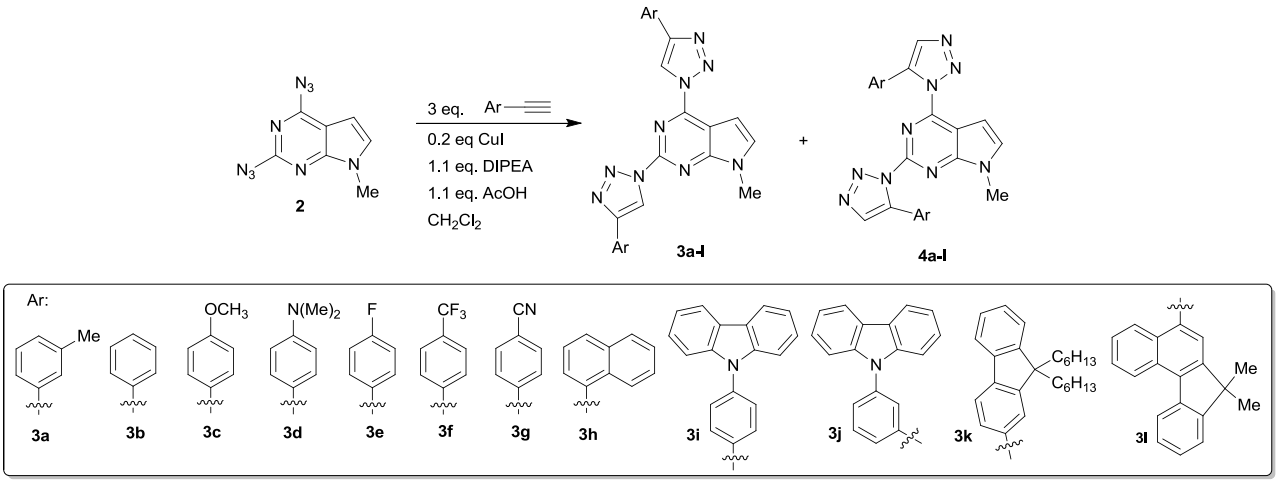

Entry	Reaction time, h	Regioisomeric ratio (**3**:**4**)[a]	Overall yield[b] (**3**+**4**), %	Yield,[c] %
1	72	70:30	78	46 (**3a**)
2	48	-[d]	-	48 (**3b**)
3	72	83:17	79	58 (**3c**)
4	72	63:37	74	35 (**3d**)
5	12	-[d]	-	61 (**3e**)
6	12	95:5	89	79 (**3f**)
7	8	-[d]	-	75 (**3g**)
8	120	79:21	68	38 (**3h**)
9	144	85:51	62	53 (**3i**) 9 (**4i**)
10	96	90:10	78	43 (**3j**)
11	96	-[d]	-	56 (**3k**)
12	120	-[d]	-	60 (**3l**)

[a] Determined from the ^{1}H NMR spectra of obtained isomeric mixture. [b] Yield of crude mixture of isomers. [c] Isolated yield. [d] Formation of compounds **4** was not observed.

However, in the reaction of **2** with phenyl-, *p*-fluorophenyl, *p*-cianophenyl, 9,9-dihexyl-2-fluorenyl- and 7,7-dimethylbenzo[*c*]fluoren-5-ylethynes formation of 1,5-disubstituted triazoles was not detected by NMR technique (Table 3, entries 2, 5, 7, 11, 12). Due to similar R_f values of isomeric triazoles **3** and **4** mixtures could not be separated into both individual isomers by column chromatography. Only one pure 1,5-disubstituted triazole **4i** was isolated in 9% yield (Table 3, entry 9). Nevertheless, all major 1,4-disubstituted triazoles **3a-l** were isolated and purified by fractional crystallization of the crude mixture of isomers from 2-PrOH or toluene.

Molecular Orbital Calculations and Cyclic Voltammetry

To gain insight into the effect of various substituents on the geometrical and electronic properties of the chromophores density functional theory (DFT) calculations were carried out on the synthesized compounds **3a-l** by using Gaussian 09 program package.[23] The geometries of compounds were optimized using B3LYP exchange-correlation hybrid functional together with the 6-311G** basis set. To get correctly optimized structures potential energy surface scan of dihedral angle at the position 4 of the pyrrolo[2,3-*d*]pyrimidine was performed with a step of 5 degrees. The scan revealed two local minima at dihedral angle at 40° and 320° degrees and global minimum positioned at coplanar geometry with *anti*-orientation of the 1,2,3-triazole ring (Figure 2). 1,2,3-Triazole ring at the position 2 of the heterocycle can accept *syn*- or *anti*-conformation (in respect of the pyrrolo[2,3-*d*]pyrimidine ring). Potential energy comparison of both structures indicated that *anti-anti* conformation of triazole rings is energetically more favored than *anti-syn* conformation by 0.64 kcal/mol (Figure 2).

Examination of geometry of the optimized structures of the studied systems revealed that compounds possessing phenyl substituent at 1,2,3-triazole linker are almost coplanar (**3a-g, 3k**), while compounds with more bulky aryl fragments exhibit twisted geometry. For molecules **3h** and **3l,** naphthyl and benzofluorenyl fragments are out of plane of the rest of the molecule (dihedral angle 34.4° – 36.3°) and for **3i, j** carbazolyl moieties are twisted by 57.4° - 58.6°.

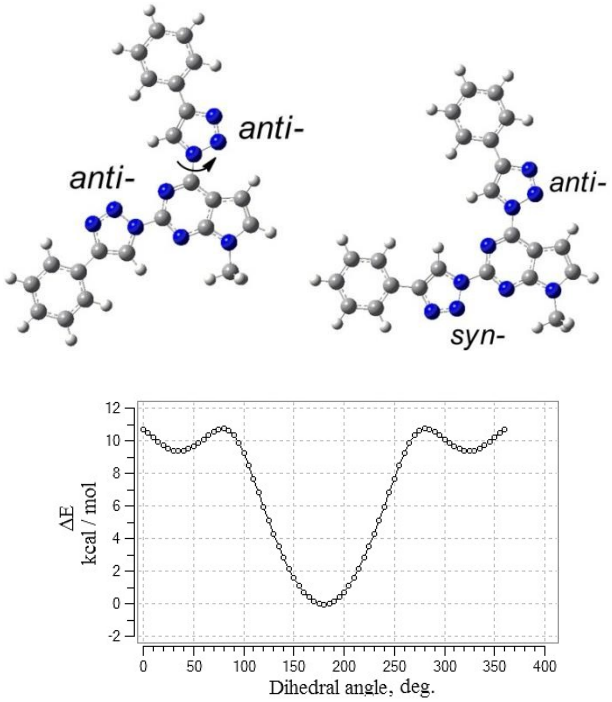

Figure 2. *Anti-anti, anti-syn* conformations and potential energy surface scan of compound **3b**.

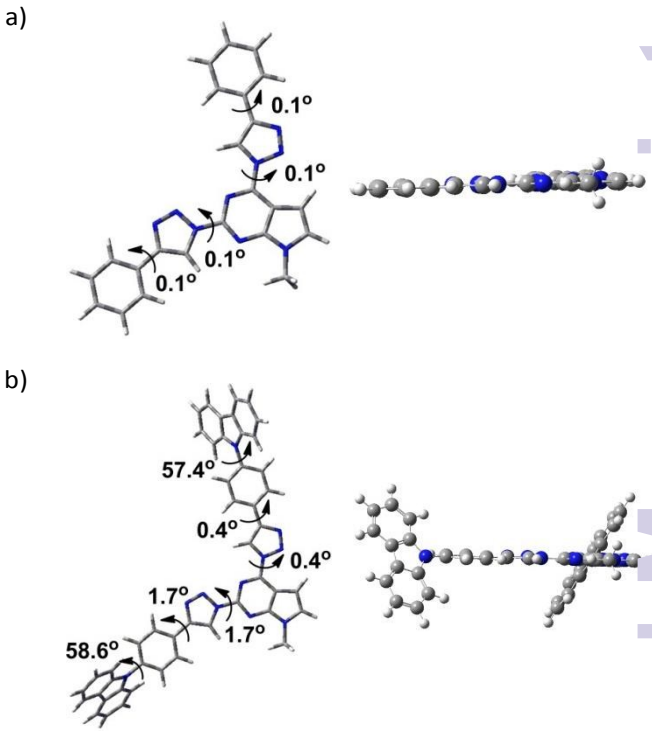

Figure 3. Optimized structure geometries a) compound **3b**; b) compound **3i**.

Optimised structures of compounds **3b** and **3i** are given in Figure 3 (see supporting information for the rest compounds).

The DFT computed localization of frontier molecular orbitals (FMOs) of compounds **3a-l** is presented in Figure 4. A comparison of electronic structures revealed that the LUMO of all the homologues is localized on pyrrolo[2,3-*d*]pyrimidine core involving conjugated co-planar 1,2,3-triazolyl moieties. The main difference of the electronic structure is revealed in the HOMO state. For molecules possessing small slightly electron-donating substituents (**3a-b**) or electron-withdrawing substituents (**3e-g**) HOMO is localized over the entire molecule, enclosing the pyrrolo[2,3-*d*]pyrimidine core. Introduction of substituents with increasing electron-donating properties (**3c-d**) results in enhanced intramolecular charge transfer. On the other hand, the introduction of bulky naphthyl (**3h**), carbazolyl (**3i-j**) and benzo[*c*]fluorenyl (**3l**) fragments, resulting in twisted geometry of the molecules, yields non-symmetric localization of the HOMO on the sole substituent attached at the position 4 of the pyrrolopyrimidine moiety and thus, manifests strong intramolecular charge transfer character. Compound **3k** possessing bulky fluorene moieties and nevertheless, showing planar geometry exhibits intermediate properties of HOMO localization, comprising both substituents at the 2nd and 4th positions of the pyrimidine ring and partially extending to the pyrrolo[2,3-*d*]pyrimidine core.

Comparison of calculated energies of FMO's for compounds **3a-g** revealed the impact of polar substituents (Figure 5). The energy of the HOMO level steadily decreases from -5.08 eV to -6.69 eV going from the most electron-donating substituents to the most electron-withdrawing substituents (compound **3d** and compound **3e**, respectively). The energy of the LUMO state also steadily decreases with substituent polarity from -1.95 eV to -2.71 eV. The resulting energy gap increases from 3.13 eV to 4.04 eV. Incorporation of the bulky substituents (Fig. 5) results in the increase of the HOMO energy with increasing size of aryl substituents (from -5.85 eV to -5.5 eV for compounds **3h** and **3l**). The energy of the LUMO state slightly decreases with increasing size of the conjugated system from - 2.24 eV to -2.29 eV, thus the corresponding band gap decreases from 3.61 eV to 3.21 eV.

The cyclic voltammetry (CV) measurements were carried out with a glassy carbon electrode in DCM or DMF solutions containing 0.10 M tetrabutylammonium hexafluorophosphate as electrolyte and Ag/Ag^{+} as the reference electrode at the 50 mV/s scan rate. Each measurement was calibrated with ferrocene as internal standard. The LUMO energies were calculated from the first signal onset of reduction using formula LUMO = $-(1.19 \cdot E(red)_{onsvsFc}+4.78)$.[24] All compounds exhibited one irreversible reduction wave. HOMO values were calculated from the optical band gaps and LUMO values using formula $E_{HOMO} = E_{Lumo} - E_g^{opt}$. Typical voltammogram of compound **3e** is shown in Figure 6 (for compounds **3a-d** and **3g-l** see supporting information).

Compd.	*HOMO*	*LUMO*	Compd	*HOMO*	*LUMO*
3a	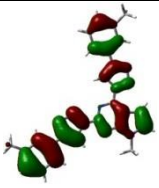	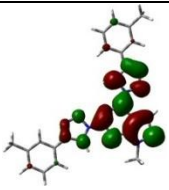	**3b**	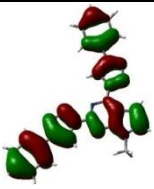	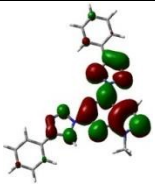
	-6.10 eV	-2.21eV		-6.18 eV	-2.25 eV
3c	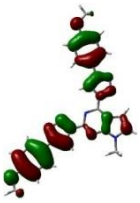	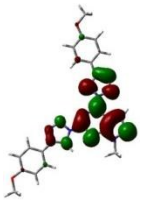	**3d**	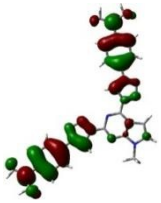	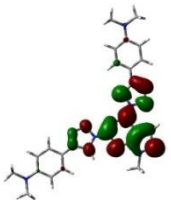
	-5.71 eV	-2.12 eV		-5.08 eV	-1.95 eV
3e	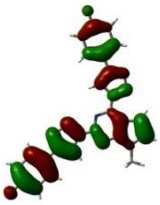	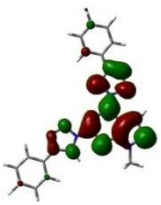	**3f**	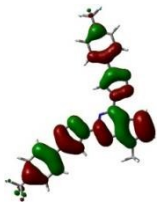	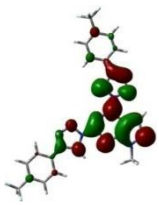
	-6.23 eV	-2.35 eV		-6.60 eV	-2.56 eV
3g	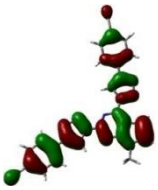	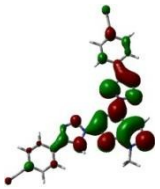	**3h**	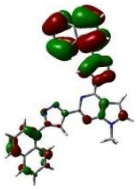	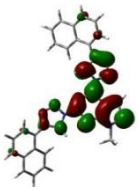
	-6.69 eV	-2.71 eV		-5.85 eV	-2.24 eV
3i	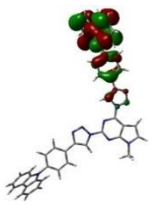	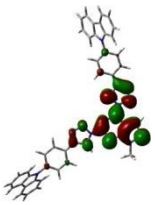	**3j**	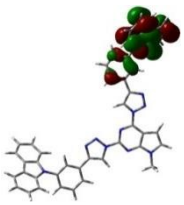	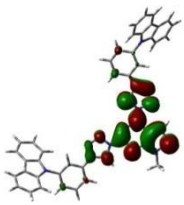
	-5.54 eV	-2.42 eV		-5.52 eV	-2.42 eV
3k	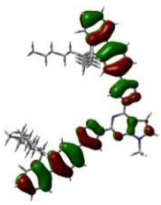	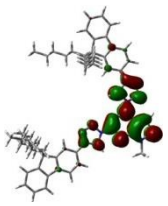	**3l**	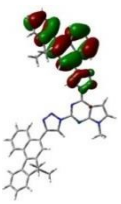	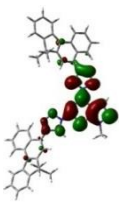
	-5.71 eV	-2.23 eV		-5.50 eV	-2.29 eV

Figure 4. Calculated spatial distributions of HOMO and LUMO of compounds **3a-l**.

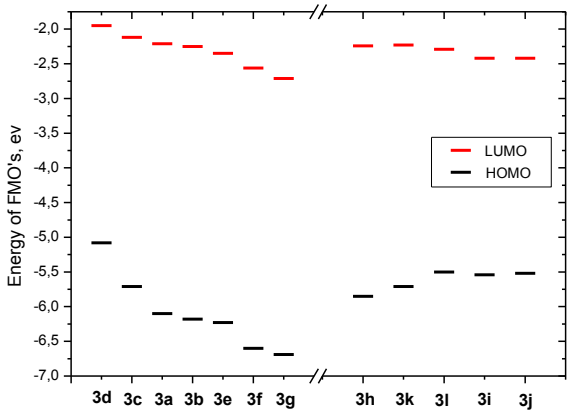

Figure 5. Diagram of calculated FMOs energy values of compounds **3a-l**

The obtained data of CV measurements are summarized in Table 4. Variation of the experimentally obtained values induced by electronic effects of substituents is significantly smaller due to an opposite effect resulting from the polarity of the surrounding media. Note, that the cyclic voltammetry results were obtained in dichloromethane or in highly polar DMF surrounding, in contrast to the theoretical calculations simulating vacuum conditions. Thus, the shift of the LUMO level energy induced by substituent polarity is, probably, diminished by the solvatic shift of energy levels (Table 4).

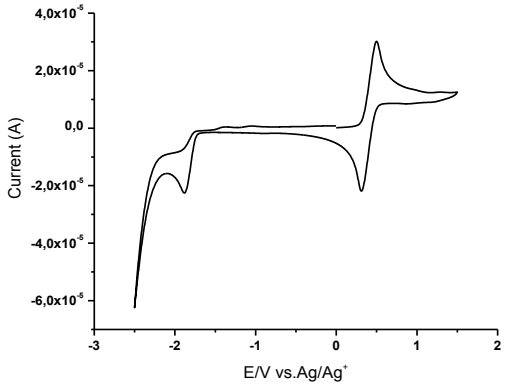

Figure 6. Typical voltammogram of compound **3e**

Optical Properties

Optical properties of the synthesized compounds **3a-l** were assessed by performing absorption and fluorescence spectroscopy, fluorescence lifetime and fluorescence quantum yield measurements in $CHCl_3$, THF and DMF solutions. Absorption and fluorescence data of 2,4-bis(4-aryl-1,2,3-triazol-1-yl)pyrrolo[2,3-*d*]pyrimidines (**3a-l**) are collected in Table 6. The studied compounds exhibit strong UV absorption in dilute solutions with their absorption maxima positioned in a region from 245 to 365 nm. Most of the synthesized compounds show two specific absorption bands located at around 260 nm and 310 nm, characteristic to pyrrolo[2,3-*d*]pyrimidine units (not observed in DMF because of UV cut-off value 268 nm).[25]

Table 4. Experimentally obtained HOMO and LUMO values of compounds **3a-l**.

Compound	E_{LUMO}, eV[a]	E_{HOMO}, eV[b]	E_g^{opt}, eV[c]
3a[d]	-2.16	-5.54	3.38
3b[d]	-2.18	-5.58	3.40
3c[d]	-2.24	-5.50	3.26
3d[d]	-2.17	-5.04	2.87
3e[d]	-2.23	-5.60	3.37
3f[d]	-[e]	-[e]	3.35
3g[d]	-2.30	-5.72	3.42
3h[f]	-2.30	-5.67	3.37
3i[f]	-2.34	-5.59	3.25
3j[f]	-2.35	-5.7	3.35
3k[d]	-2.64	-5.96	3.32
3l[d]	-2.26	-5.40	3.14

[a]Calculated by the formula:$E_{LUMO} = -(1.19 \cdot E(red)_{onsvsFc} + 4.78)$. [b]Calculated by the formula: $E_{HOMO} = E_{Lumo} - E_g^{opt}$. [c]Obtained from the intersection of UV/vis and fluorescence spectra. [d] CV measurements were performed in CH_2Cl_2. [e] Could not be measured because of very low solubility. [f] CV measurements were performed in DMF.

Compounds **3c-d**, possessing electron donating substituents show decreasing oscillator strength and a red-shift of the lowest energy absorption band, which is attributed to the ICT behaviour, in accordance with quantum chemical calculations. Strong electron-donating dimethylamino group (compound **3d**) caused a red shift of the absorption bands to 365 nm. The absorption spectra of compounds **3i-j**, bearing bulky carbazole fragments show absorption bands at 290 nm and 340 nm, which are assigned to the carbazolyl moieties.[26] Solvent polarity has no significant influence on the absorption maxima of the studied compounds indicating small dipole moment in the ground state.

All compounds possessing substituted phenyl fragments show broad structureless fluorescence spectra in the region from 402 nm to 649 nm depending on the electronic nature of the substituents and the polarity of the surrounding media. The normalized absorption and fluorescence spectra of compounds **3b-d** in $CHCl_3$, THF, DMF are presented in Figure 7 (see Supporting Information for compounds **3a**, **3e-l**). Weak λ_{em} dependence on solvent polarity in the range from 402 nm to 436 nm was observed for compounds bearing phenyl, *m*-tolyl and electron-withdrawing substituents in a *para*-position of aromatic rings of the 2,4-bis(triazolyl)pyrrolo[2,3-*d*]pyrimidines (**3a,b**, **3e-g)**.

However, incorporation of electron-donating methoxy (compound **3c**) group results in broadening of fluorescence spectra. Moreover, dimethylamino substituent (compound **3d**) results in prominent red-shift from 402 nm up to 530 nm. Thus, broadening and enhanced Stokes shift from 91 nm (**3b** in $CHCl_3$) to 165 nm (**3d** in $CHCl_3$) of the fluorescence spectra, this is due to the strong charge transfer character of the excited state. In accordance with the CT nature of the transitions the enhancement of surrounding media polarity results in even higher red-shift of the fluorescence spectra up to 650 nm and increased Stokes shift – 279 nm

Table 6. Optical properties of compounds **3a-l**.

		3a	3b	3c	3d	3e	3f	3g	3h	3i	3j	3k	3l
$CHCl_3$	λ_{abs},nm	255 309	264 311	268 318	308 365	249 312	253 310	277 311	245 298	247 293 313 329	253 293 314 326	245 293 319	246 334 348
	λ_{em},nm	402	402	405	530	403	404	408	404	341 453	340 454	422	459
	Φ_F,%[a]	52	49	27	52	49	44	52	27	55	6	34	28
	Stokes shift, nm	93	91	87	165	91	93	97	106	112	114	103	111
	τ, ns	5.2	5.4	2.9	12.3	5.8	6.7	6.4	3.5	9.0	17.8 (86%) 3.4 (10%) 0.1 (4%)	2.6	3.3
	τ_R, ns[b]	10.9	10.7	8.7	23.6	11.4	12.0	13.4	4.7	16.4	-	7.6	11.9
	τ_{NR}, ns[b]	10.0	11.1	4.2	25.6	11.9	15.3	12.4	12.8	20.0	-	3.9	4.6
THF	λ_{abs},nm	256 309	262 309	266 321	310 366	250 312	255 312	270 290	247 297	249 295 312 324	251 295 312 328	246 293 320	246 334 348
	λ_{em},nm	416	417	418	569	418	422	422	418	342 459	341 422	417	455
	Φ_F,%[a]	55	73	31	38	61	43	67	32	50	17	32	25
	Stokes shift, nm	107	108	97	203	106	110	132	121	117	81	97	107
	τ, ns	7.3	7.5	3.8	9.8	7.8	7.8	7.5	5.5	8.7	15.2 (71%) 1.3 (17%) 0.3 (12%)	3.0	3.7
	τ_R, ns[b]	13.2	10.3	12.2	25.9	12.8	18.2	11.1	17.1	17.6	-	9.3	14.8
	τ_{NR}, ns[b]	16.1	27.8	5.5	15.9	20.0	13.7	22.8	8.0	17.6	-	4.4	4.9
DMF	λ_{abs},nm	311	311	320	309 370	311	314	279 312	299	298 315 330	297 316 326	295 324	335 348
	λ_{em},nm	424	423	436	650	431	436	435	432	345 530	346 435	436	492
	Φ_F,%[a]	71	62	21	3	56	50	56	31	27	5	41	19
	Stokes shift, nm	113	112	116	279	120	122	123	133	185	89	112	144
	τ, ns	7.3	9.8	6.3	2.2	10.4	10.6	9.8	7.7	12.5 (74%) 20.4 (26%)	1.8 (44%) 0.5 (56%)	6.3	4.8
	τ_R, ns[b]	10.2	15.8	30.2	75.0	18.5	21.2	17.6	24.9	-	-	15.4	25.5
	τ_{NR}, ns[b]	25.1	25.8	8.0	2.3	23.6	21.2	22.3	11.2	-	-	10.7	6.0

[a]Φ_F values obtained by the integrated sphere method with 4% error are provided. [b]Radiative and non-radiative decay time constants are calculated as τ/Φ_F and $\tau/(1-\Phi_F)$, respectively.

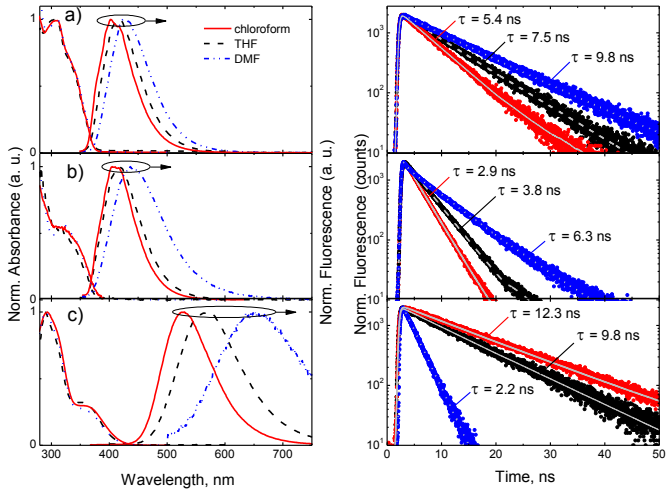

Figure 7. Normalized absorption and fluorescence spectra (left) and fluorescence decay profiles (right) of compounds **3b** (a), **3c** (b) and **3d** (c) in chloroform, THF and DMF solutions (c = 10^{-5} M).

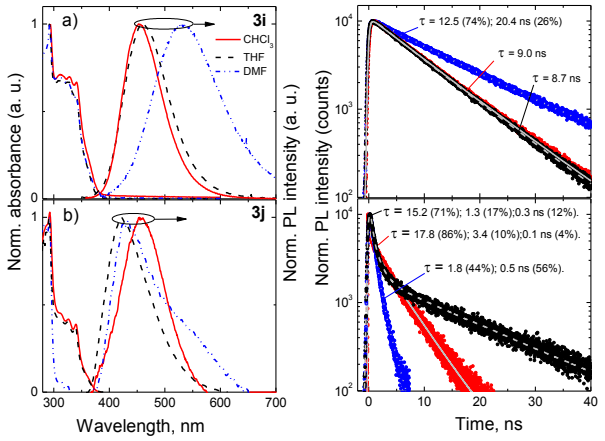

Figure 8. Normalized absorption and fluorescence spectra (left) and fluorescence dec profiles (right) of compounds **3i** (a) and **3j** (b) in chloroform, THF and DMF solutions (c = 10^{-5} M).

Compounds **3h**, **3k** and **3l** bearing naphthyl, fluorenyl and benzofluorenyl fragments show steady red-shifting of the fluorescence bands from 402 nm to 459 nm in the solvent of low polarity, due to extension of π-conjugated system. All these compounds show minor solvatochromic changes with increasing polarity of the surrounding media. Compound **3i**, bearing bulky electron donating carbazole moiety, shows red-shifted broad fluorescence band at 453 nm in chloroform and at 530 nm in polar DMF. Interestingly, its isomer - compound **3j**, bearing carbazole fragment at the *meta*-position of the benzene ring, reveals the dual-fluorescence properties in polar DMF surrounding showing both locally excited band at 435 nm, typical for non-polar media, and an additional CT band at around 550 nm (Figure 8).

Most of the compounds demonstrated efficient blue fluorescence with quantum yields up to 71%. Compounds bearing neutral and electron-withdrawing substituents (**3a-b**, **3e-g**) demonstrated fluorescence quantum yields varying from 44% to 52% in solvent of low polarity ($CHCl_3$), while the higher polarity of the surrounding media results in slightly higher efficiencies from 50% to 71%. Much more prominent variation depending on solvent polarity is observed for the excitation relaxation rates. The single exponential profiles of the decay transients enabled the estimation of radiative and non-radiative decay lifetimes. For compounds **3a-b**, **3e-g,** both the radiative and non-radiative decay lifetimes show almost two-fold increase in polar DMF solvent, as compared to less polar chloroform, which is evident by significant slowdown of the fluorescence decay transients (see figure 7). The prominent variation of both radiative and non-radiative decay lifetimes indicates on charge transfer induced intramolecular twisting reactions, determined by solvation shell.[27] This effect is even more evident for compounds **3c** and **3d** bearing electron donating substituents, with pronounced intramolecular charge transfer. Here, the radiative decay lifetimes increase more than 3 times in the solutions of polar DMF, while in the case of compounds with non-polar and electron withdrawing moieties, with less pronounced CT nature, the increase of the radiative decay lifetime was about 30%. The non-radiative decay rates are 2 or 3 times higher in the polar surrounding for all the compounds, with the exception of dimethylamino group bearing compound **3d**, where the non-radiative decay rate undergoes a 10-fold increase in polar surrounding. Thus, the resulting fluorescence quantum yield of differently substituted derivatives, comprising electron deficient pyrrolo[2,3-*d*]pyrimidine core, depends on competition between both, decreased radiative and non-radiative decay rates.

Compounds **3h-k** bearing non-polar bulky aryl substituents revealed similar trends of solvent polarity dependencies of the radiative and non-radiative decay rates. Two-fold increase of the radiative decay lifetime accompanied by the significant increase of the non-radiative decay lifetime from 1.5 to 2.5 times results in slightly lower fluorescence quantum yields ranging from 19% to 41%. Incorporation of electron donating carbazole units at the *para*-position of the phenyl fragments (compound **3i**) results in the fluorescence quantum yield of 55%, which decreases to 27% in polar surroundings. Interestingly, the attachment of the carbazole unit at the meta position of the phenyl fragment (compound **3j**) results in a dramatic decrease of the fluorescence efficiency to 6%, which might be attributed to the broken symmetry of donor and acceptor moieties, resulting in dual-fluorescence nature of the excited states, prominent not only in the fluorescence spectra but also in the non-exponential decay transients in both non-polar and polar surrounding media.

Conclusions

In summary, novel D-π-A-π-D type chromophores - 2,4-bis(4-aryl-1,2,3-triazol-1-yl)pyrrolo[2,3-*d*]pyrimidines were prepared by CuAAC reaction of 2,4-diazido-7-methylpyrrolo[2,3-*d*]pyrimidine with diverse ethynylarenes at room temperature in dichloromethane using CuI/DIPEA/AcOH

catalyst system. It was demonstrated that in the CuAAC reaction of 2,4-diazidopyrrolo[2,3-*d*]pyrimidine along with 1,4-disubstituted 1,2,3-triazoles some amounts of 1,5-disubstituted isomers were formed. The synthesized 2,4-bis(4-aryl-1,2,3-triazol-1-yl)pyrrolopyrimidines exhibit efficient fluorescence in the range from 402 nm to 650 nm. The introduction of various substituents enables tuning of HOMO and LUMO energies: the attachment of polar substituents in the para position of phenyl group with increasing electron-donating character results in lower HOMO and LUMO energies (from -6.69 eV to -5.08 eV for HOMO and from -2.71 eV to -1.95 eV for LUMO), while the addition of more bulky aryl substituents caused the reduction of HOMO energy (from -5.85 eV to -5.50 eV). The DFT calculations revealed that LUMO of all the derivatives are located on the pyrrolo[2,3-*d*]pyrimidine moiety and includes triazole fragments. This leads to the extension of the LUMO localization and enhanced electron-accepting properties of heterocyclic part of molecules. The bulky aryl substituents show mostly electron donating character and influence the energy levels of HOMO state. Variation of the size, polarity and geometry of the substituents alters the charge transfer character of the transitions, influencing the properties of the fluorescence spectra and fluorescence quantum yield. Intramolecular charge transfer has a considerable influence on the dynamics of radiative and non-radiative decay in polar surroundings. Both processes slow down and the competition between the radiative and non-radiative decay pathways results in smaller fluorescence quantum yields for compounds possessing electron-donating substituents or substituents with twisted geometry. The highest quantum yield of 73% was observed for a pyrrolo[2,3-*d*]pyrimidine derivative **3b** with non-polar methyl group in medium polarity solvent - THF. Compound **3d** bearing strong electron-donating dimethylamino group exhibited the largest Stokes shift of 279 nm in DMF solution.

The synthesized novel D-triazole-A-triazole-D chromophores show potential for applications as blue emitters in OLED technologies, while the sensitivity of their emission properties to the polarity of surrounding media implies potential applications for biomaterial labeling and metal ions sensing.

Experimental section

General remarks

Melting points were determined in open capillaries with a digital melting point IA9100 series apparatus (ThermoFischer Scientific). All reactions and purity of the synthesized compounds were monitored by TLC using Silica gel 60 F_{254} aluminum plates (Merck). Visualization was accomplished by UV light. Column chromatography was performed using Silica gel 60 (0.040-0.063 mm) (Merck). NMR spectra were recorded on a Bruker Ascend 400 spectrometer (400 MHz and 100 MHz for ^{1}H and ^{13}C, respectively). ^{1}H NMR and ^{13}C NMR were referenced to residual solvent peaks. Infrared spectra (IR) were recorded on an IR spectrophotometer Spectrum BX II (Perkin Elmer). High Resolution Mass Spectrometry (HRMS) analyses were carried out on a quadrupole, time-of-flight mass spectrometer (microTOF-Q II, Bruker Daltonik GmbH, Bremen, Germany) or on Dual-ESI Q-TOF 6520 (Agilent Technologies) mass spectrometers. All quantum chemical calculations were carried out using Gaussian 09 program package. Geometries were optimized at DFT/B3LYP/6-311G** level of theory. Structures for calculations of shielding values were further optimized by applying self-consistent reaction field (SCRF) under the polarizable continuum model (IEFPCM) incorporating DMSO as solvent, absolute shielding values were calculated by GIAO method. TMS was used as a reference in calculating ^{1}H and ^{13}C chemical shifts from absolute shielding values. Electrochemical investigation was carried out using BioLogic SAS and a micro-AUTOLAB Type III potentiostat-galvanostat. The solutions of the synthesized compounds with the concentration of 10^{-5} M were used for cyclic voltamperometry (CV) measurements. The experiments were calibrated with the standard ferrocene/ferrocenium redox system. The absorption spectra were recorded on a Perkin Elmer UV-vis-NIR spectrophotometer Lambda 950. Fluorescence of the sample solutions was excited by 320 nm wavelength light-emitting diode and measured using back-thinned CCD spectrometer (Hamamatsu PMA-11). The fluorescence quantum yield (Φ_F) of the solutions was estimated by comparing wavelength-integrated fluorescence intensity of the solution with that of the reference. Quinine sulfate in 0.1M H_2SO_4 was used as a reference. Optical densities of the reference and the sample solutions were ensured to be below 0.05 to avoid reabsorption effects. Estimated quantum yield was verified by using an alternative method of an integrating sphere (Sphere Optics), which was coupled to the CCD spectrometer by an optical fiber. The obtained Φ_F values measured by both methods coincide within 4% error. The fluorescence quantum yield values obtained by the integrated sphere method are provided in Table 6. Fluorescence transients of the sample solutions were measured using time-correlated single photon counting system (PicoQuant PicoHarp 300).

2,4-diazido-7-methylpyrrolo[2,3-d]pyrimidine 2

A mixture of compound **1**[28] (1.0 g, 4.95 mmol) and NaN_3 (0.708 g, 10.89 mmol) in DMF (35 mL) was stirred at room temperature for 24 hrs. Then the reaction mixture was poured into water (100 mL). Precipitate was filtered off, washed with MeOH, dried at room temperature and stored in a vessel protected from sunlight. Product obtained as white solid (0.83 g, 78%), mp 118-119°C dec. ^{1}H NMR (400 MHz, $CDCl_3$): δ = 3.80 (3H, s, NCH_3), 6.51 (1H, d, *J* = 3.6 Hz, 5-H), 7.00 (1H, d, *J* = 3.6 Hz, 6-H); ^{13}C NMR (100 MHz, $CDCl_3$): δ = 31.6, 99.0, 105.7, 128.5, 153.6, 155.13, 155.14; IR (KBr): 2152 cm^{-1} (N_3), 2115 cm^{-1} (N_3); HRMS (ESI): calculated for $C_7H_5N_9Na$ $[M+Na]^+$ = 238.0560, found 238.0560.

General procedure for the synthesis of compounds 3a-l

A mixture of compound **2** (100 mg, 0.46 mmol), corresponding alkyne (1.4 mmol), CuI (17 mg, 0.09 mmol), DIPEA (89 µL, 0.51 mmol) and acetic acid (29 µL, 0.51 mmol) in CH_2Cl_2 (5 mL) was stirred at room temperature. End of the reaction was monitored by TLC. Then the reaction mixture was poured into water (20 mL) and extracted with CH_2Cl_2 (3x10 mL). The extracts were combined, dried over Na_2SO_4 and filtered. After removal of the solvent the residue was purified by column chromatography on silica gel (eluent - hexane/EtOAc) to give a crude isomeric mixture. Compounds **3a-l** were purified by recrystallization from 2-PrOH or toluene.

7-Methyl-2,4-bis(4-(*m*-tolyl)-1*H*-1,2,3-triazol-1-yl)-7*H*-pyrrolo[2,3-*d*]pyrimidine (3a)

White solid (94 mg, 46%); mp 220 °C dec. (from 2-PrOH); λ_{max} ($CHCl_3$)/nm 255 and 309 (ε/dm^{-3}mol^{-1}cm^{-1} 15104 and 8320). ^{1}H NMR (400 MHz, $CDCl_3$): δ 2.49 (6H, s, 2xCH_3), 4.07 (3H, s, NCH_3), 7.22-7.30 (2H, m, ArH), 7.40-7.48 (3H, m, ArH, 5-H), 7.49 (1H, d, *J* = 3.6 Hz, 6-H), 7.84 (2H, t, *J* = 8.8 Hz, ArH) 7.90 (2H, s, ArH), 8.91 (1H, s, triazole-H), 9.14 (1H, s, triazole-H). ^{13}C NMR (100 MHz, $CDCl_3$): δ 21.4, 31.9, 103.2, 106.9, 117.5, 118.3, 123.11, 123.16, 126.6, 126.7, 128.7, 128.9, 129.34, 129.36 129.6, 129.8, 132.3, 138.6, 138.7, 147.1, 147.6, 147.7, 147.9, 154.1. HRMS (ESI): calculated for $C_{25}H_{21}N_9Na$ $[M+Na]^+$ = 470.1812; found: 470.1824.

7-Methyl-2,4-bis(4-phenyl-1*H*-1,2,3-triazol-1-yl)-7*H*-pyrrolo[2,3-*d*]pyrimidine (3b)

White solid (92 mg, 48%); mp 237 °C dec. (from 2-PrOH); λ_{max} ($CHCl_3$)/nm 264 and 311 (ε/dm^{-3}mol^{-1}cm^{-1} 8784 and 7798). ^{1}H NMR (400 MHz, $CDCl_3$): δ 4.07 (3H, s, NCH_3), 7.42-7.47 (3H, m, ArH, 5-H), 7.49 (1H, d, *J* = 3.6 Hz, 6-H), 7.51-7.56 (4H, m, ArH), 8.04-8.07 (4H, m, ArH), 8.93 (1H, s, triazole-H), 9.14 (1H, s, triazole-H). ^{13}C NMR (100 MHz, $CDCl_3$): δ 32.0, 103.4, 107.4, 117.7, 118.5, 126.11, 126.14, 128.6, 128.91, 128.94, 129.1, 129.6, 130.1, 132.5, 147.4, 147.8, 147.9, 148.0, 154.3. HRMS (ESI): calculated for $C_{23}H_{17}N_9$ $[M+H]^+$ = 420.1680; found: 420.1694.

2,4-Bis[4-(4-methoxyphenyl)-1*H*-1,2,3-triazol-1-yl]-7-methyl-7*H*-pyrrolo[2,3-*d*]pyrimidine (3c)

Yellow solid (128 mg, 58%); mp 247 °C dec. (from toluene); λ_{max} ($CHCl_3$)/nm 268 and 318 (ε/dm^{-3}mol^{-1}cm^{-1} 7060 and 5585). ^{1}H NMR (400 MHz, $CDCl_3$): δ 3.91 (3H, s, OCH_3), 3.91, (3H, s, OCH_3), 4.06 (3H, s, NCH_3), 7.06 (2H, d, *J* = 8.8 Hz, ArH), 7.07 (2H, d, *J* = 8.8 Hz, ArH), 7.42 (1H, d, *J* = 3.6 Hz, 5-H), 7.48 (1H, d, *J* = 3.6 Hz, 6-H), 7.97 (2H, d, *J* = 8.8 Hz, ArH), 7.99 (2H, d, *J* = 8.8 Hz, ArH), 8.84 (1H, s, triazole-H), 9.07 (1H, s, triazole-H). ^{13}C NMR (100 MHz, d_6-DMSO, 80°C): δ 32.1, 55.8, 102.0, 106.8, 114.9, 115.0, 118.6, 119.8, 122.6, 123.1, 127.5, 127.7, 134.6, 146.9, 147.31, 147.8, 147.64, 154.5, 160.1, 160.3. HRMS (ESI): calculated for $C_{25}H_{22}N_9O_2$ $[M+H]^+$ = 480.1891; found: 480.1905.

2,4-Bis[4-(4-dimethylaminophenyl)-1*H*-1,2,3-triazol-1-y]-7-methyl-7*H*-pyrrolo[2,3-*d*]pyrimidine (3d)

Yellow solid (81 mg, 35%); mp 225 °C dec. (from toluene); λ_{max} ($CHCl_3$)/nm 308 and 365 (ε/dm^{-3}mol^{-1}cm^{-1} 14827 and 6182). ^{1}H NMR (400 MHz, $CDCl_3$): δ 3.03 (6H, s, $N(CH_3)_2$), 3.05 (6H, s, $N(CH_3)_2$), 4.02 (3H, s, NCH_3), 6.81 (2H, d, *J* = 8.8 Hz, ArH), 6.84 (2H, d, *J* = 8.8 Hz, ArH), 7.35 (1H, d, *J* = 3.2 Hz, 5-H), 7.43 (1H, d, *J* = 3.2 Hz, 6-H), 7.87 (2H, d, *J* = 8.8 Hz, ArH), 7.90 (2H, d, *J* = 8.8 Hz, ArH), 8.72 (1H, s, triazole-H), 8.94 (1H, s, triazole-H). ^{13}C NMR (100 MHz, d_6-DMSO, 80°C): δ 31.8, 40.41, 40.43, 103.4, 106.9, 112.3, 112.4, 115.7, 116.7, 117.5, 118.1, 127.0, 127.1, 132.0, 147.4, 147.9, 148.1, 148.3, 150.6, 150.7, 154.1. HRMS (ESI): calculated for $C_{27}H_{28}N_{11}$ $[M+H]^+$ = 506.2524; found: 506.2536.

2,4-Bis[4-(4-fluorophenyl)-1*H*-1,2,3-triazol-1-y])-7-methyl-7*H*-pyrrolo[2,3-*d*]pyrimidine (3e)

White solid (127 mg, 61%); mp 232 °C dec. (from 2-PrOH); λ_{max} ($CHCl_3$)/nm 249 and 312 (ε/dm^{-3}mol^{-1}cm^{-1} 19602 and 7777). ^{1}H NMR (400 MHZ, $CDCl_3$): δ 4.02 (3H, s, NCH_3), 7.20 (4H, m, ArH), 7.38 (1H, d, *J* = 3.6 Hz, 5-H), 7.41 (1H, d, *J* = 3.6 Hz, 6-H), 7.98 (4H, m, ArH), 8.82 (1H, s, triazole-H)), 9.04 (1H, s, triazole-H). ^{13}C NMR (100 MHz, $CDCl_3$): δ 31.9, 103.9, 107.0, 115.9 (d, *J* = 21Hz), 116.1 (d, *J* = 21Hz), 117.4, 118.1, 125.7 (d, *J* = 4Hz), 126.2 (d, *J* = 4Hz), 127.8 (d, *J* = 8Hz), 127.9 (d, *J* = 8Hz), 132.5, 146.8, 147.10, 147.16, 147.6, 154.1, 162.9 (d, *J* = 247Hz), 163.1 (d, *J* = 247Hz). HRMS (ESI): calculated for $C_{23}H_{15}F_2N_9Na$ $[M+Na]^+$ = 478.1311; found: 478.1321.

7-Methyl-2,4-bis[4-(4-trifluoromethylphenyl)-1*H*-1,2,3-triazol-1-yl]-7*H*-pyrrolo[2,3-*d*]pyrimidine (3f)

Compound **3f** was filtered from the reaction mixture and washed with CH_2Cl_2 and water. Obtained as yellow solid (201 mg, 79%); mp 228 °C dec. (from toluene); λ_{max} ($CHCl_3$)/nm (ε/dm^{-3}mol^{-1}cm^{-1} 19761 and 8730). ^{1}H NMR (400 MHz, $CDCl_3$): 4.09 (3H, s, NCH_3), 7.47 (1H, d, *J* = 3.6 Hz, 5-H), 7.50 (1H, d, *J* = 3.6 Hz, 6-H), 7.78-7.81 (4H, m, ArH), 8.17 (2H, d, *J* = 8.0 Hz, ArH) 8.19 (2H, d, *J* = 8.0 Hz, ArH), 9.01 (1H, s, triazole-H), 9.26 (1H, s, triazole-H). ^{13}C NMR could not be obtained because of very low solubility in common deuterated solvents. HRMS (ESI): calculated for $C_{25}H_{15}F_6N_9Na$ $[M+Na]^+$ = 578.1247; found: 578.1248.

7-Methyl-2,4-bis[4-(4-cianophenyl)-1*H*-1,2,3-triazol-1-yl]-7*H*-pyrrolo[2,3-*d*]pyrimidine (3g)

White solid (162 mg, 75%); mp 274 °C dec. (from toluene); λ_{max} ($CHCl_3$)/nm 277 and 311 (ε/dm^{-3}mol^{-1}cm^{-1} 20300 and 10716). ^{1}H NMR (400 MHz, d_6-DMSO, 80°C): δ 4.01 (3H, s, NCH_3), 7.23 (1H, d, *J* = 3.2 Hz, 5-H), 7.86 (1H, d, *J* = 3.2 Hz, 6-H), 7.95 (4H, d, *J* = 6.8 Hz, ArH), 8.23 (4H, m, ArH), 9.62 (1H, s, triazole-H), 9.72 (1H, s, triazole-H). ^{13}C NMR (100 MHz, d_6-DMSO, 80°C): δ 32.0, 102.0, 107.3, 111.4, 111.8, 118.90, 118.96, 121.3, 122.3, 126.8, 127.0, 133.33, 133.36, 134.5, 135.0, 135.1, 145.8, 145.9, 146.7, 147.4, 154.6. HRMS (ESI): calculated for $C_{25}H_{15}N_{11}Na$ $[M+Na]^+$ = 492.1404; found: 492.1411.

7-Methyl-2,4-bis[4-(naphth-1-yl)-1*H*-1,2,3-triazol-1-yl]-7*H*-pyrrolo[2,3-*d*]pyrimidine (3h)

Yellow solid (90 mg, 38%); mp 216 °C dec. (from 2-PrOH); λ_{max} ($CHCl_3$)/nm 245 and 298 (ε/$dm^{-3}mol^{-1}cm^{-1}$ 16158 and 12867). ^{1}H NMR (400 MHz, $CDCl_3$): δ 4.07 (3H, s, NCH_3), 7.44 (1H, d, *J* = 3.6 Hz, 5-H), 7.54 (1H, d, *J* = 3.6 Hz, 6-H), 7.55-7.61 (6H, m, ArH), 7.86-7.97 (6H, m, ArH), 8.49-8.54 (2H, m, ArH), 8.96 (1H, s, triazole-H), 9.19 (1H, s, triazole-H). ^{13}C NMR (100 MHz, $CDCl_3$): δ 32.0, 103.4, 107.1, 120.7, 121.6, 125.33, 125.37,125.38, 125.4, 126.1, 126.2, 126.82, 12.97, 126.98, 127.4, 127.5, 127.6, 128.50, 128.56, 129.3, 129.5, 131.09, 131.2, 132.6, 133.92, 133.94, 147.22, 147.27, 147.3, 147.8, 154.33. HRMS (ESI): calculated for $C_{31}H_{22}N_9$ $[M+H]^+$ = 520.1993; found: 520.2005.

7-Methyl-2,4-bis{4-[4-(9-carbazolyl)phenyl]-1*H*-1,2,3-triazol-1-yl}-7*H*-pyrrolo[2,3-*d*]pyrimidine (3i)

Yellow solid (182 mg, 53%), mp 268 °C dec. (from toluene); λ_{max} ($CHCl_3$)/nm 247, 293, 313, 329 and 341 (ε/$dm^{-3}mol^{-1}cm^{-1}$ 42093, 25031, 17628, 17233 and 16471). ^{1}H NMR (400 MHz, d_6-DMSO): δ 4.04 (3H, s, NCH_3), 7.29-7.34 (5H, m, 5-H, carbazole-H), 7.45-7.52 (8H, m, ArH, carbazole-H), 7.86 (4H, t, *J* = 8 Hz, carbazole-H), 7.97 (1H, d, *J* = 3.6 Hz, 6-H), 8.28 (4H, d, *J* = 7.6 Hz, ArH), 8.38-8.43 (4H, m, carbazole-H), 9.87 (1H, s, triazole-H), 9.99 (1H, s, triazole-H). ^{13}C NMR (100 MHz, $CDCl_3$): δ 32.0, 103.4, 107.3, 109.7, 109.8, 117.9, 118.7, 120.15, 120.19, 120.41, 120.42, 123.53, 123.56, 123.61, 126.06, 126.08, 127.54, 127.59, 127.6, 128.6, 129.1, 132.7, 138.0, 138.2, 140.6, 140.7, 147.1, 147.3, 147.4, 147.7, 154.3. HRMS (ESI): calculated for $C_{47}H_{31}N_{11}Na$ $[M+Na]^+$ = 772.2656; found: 772.2659.

7-Methyl-2,4-bis{4-[3-(9-carbazolyl)phenyl]-1*H*-1,2,3-triazol-1-yl}-7*H*-pyrrolo[2,3-*d*]pyrimidine (3j)

White solid (148 mg, 43%), mp 234 °C dec (from toluene); λ_{max} ($CHCl_3$)/nm 253, 293, 314, 326 and 340 (ε/$dm^{-3}mol^{-1}cm^{-1}$ 35488, 26491, 12013, 11255 and 10549). ^{1}H NMR (400 MHz, $CDCl_3$): δ 3.98 (3H, s, NCH_3), 7.25-7.28 (5H, m, 5-H, carbazole-H), 7.36-7.46 (10H, m, carbazole-H, ArH), 7.54 (1H, d, *J* = 8.0 Hz, carbazole-H), 7.58 (1H, d, *J* = 8.0 Hz, carbazole-H), 7.68 (1H, d, *J* = 8.0 Hz, carbazole-H), 7.72 (1H, , *J* = 8.0 Hz, carbazole-H), 8.08-8.14 (6H, m, ArH, 6-H, carbazole-H), 8.23 (1H, s, ArH), 8.88 (1H, s, triazole-H); 9.12 (1H, s, triazole-H). ^{13}C NMR (100 MHz, $CDCl_3$) δ 31.9, 103.3, 107.1, 109.72,109.74, 118.2, 119.0, 120.02, 120.07, 120.24, 120.25, 123.3, 123.4, 124.57, 124.58, 124.9, 125.0, 125.9, 126.0, 127.1, 127.3, 130.5, 130.6, 131.5, 132.0, 132.5, 138.3, 138.5, 140.7, 140.8, 146.84, 146.89, 147.0, 147.3, 154.1. HRMS (ESI): calculated for $C_{47}H_{31}N_{11}Na$ $[M+Na]^+$ = 772.2656; found 772.2653

7-Methyl-2,4-bis[4-(9,9-dihexylfluoren-2-yl)-1*H*-1,2,3-triazol-1-yl]-7*H*-pyrrolo[2,3-*d*]pyrimidine (3k)

Yellow solid (240 mg, 56%) mp 102-104 °C (from 2-PrOH); λ_{max} ($CHCl_3$)/nm 245, 293 and 319 (ε/$dm^{-3}mol^{-1}cm^{-1}$ 13769, 23487 and 26245) ^{1}H NMR (400 MHz, $CDCl_3$): δ 0.67-0.79 (20H, m, $4CH_2CH_3$), 1.06-1.16 [24H, m, $4(CH_2)_3$-], 2.02-2.16 (8H, m, $4CH_2$), 4.10 (3H, s, NCH_3), 7.34-7.41 (6H, m, ArH), 7.44 (1H, d, *J* = 3.6 Hz, 5-H), 7.52 (1H, d, *J* = 3.6 Hz, 6-H), 7.77 (2H, d, *J* = 7.2 Hz, ArH); 7.85 (2H, t, *J* = 8.0 Hz, ArH), 7.99-8.08 (4H, m, ArH). 9.00 (1H, s, triazole-H), 9.24 (1H, s, triazole-H). ^{13}C NMR (100 MHz, $CDCl_3$): δ 14.0, 22.6, 23.8, 29.7, 31.5, 40.4, 40.5, 55.3, 103.4, 107.2, 117.5, 118.4, 119.8, 119.9, 120.1, 120.2, 120.42, 120.48, 122.9, 124.94, 124.95, 126.85, 126.86, 127.3, 127.4, 128.1, 128.6, 132.4, 140.5, 140.6, 141.7, 142.0, 147.4, 147.9, 148.2, 148.4, 148.6, 151.01, 151.07, 151.62, 152.67, 154.28. HRMS (ESI): calculated for $C_{61}H_{74}N_9$ [M+H] = 932.6062; found 932.6056

7-Methyl-2,4-bis[4-(7,7-dimethylbenzo[*c*]fluoren-5-yl)-1*H*-1,2,3-triazol-1-yl]-7*H*-pyrrolo[2,3-*d*]pyrimidine (3l)

Yellow solid (207 mg, 60%) mp 220 °C dec (from toluene); λ_{max} ($CHCl_3$)/nm 246, 334 and 348 (ε/$dm^{-3}mol^{-1}cm^{-1}$ 39131, 20724 and 25790). ^{1}H NMR (400 MHz, $CDCl_3$): δ 1.64 (6H, s, $2CH_3$), 1.65 (6H, s, $2CH_3$), 4.07 (3H, s, NCH_3), 7.40-7.75 (12H, m, ArH, 5-H, 6-H), 8.01 (1H, s, ArH), 8.06 (1H, s, ArH), 8.36-8.42 (2H, m, ArH), 8.54 (1H, d, *J* = 8.4 Hz, ArH), 8.61 (1H, d, *J* = 8.4 Hz, ArH), 8.84-8.90 (2H, m, ArH), 8.99 (1H, s, triazole-H), 9.25 (1H, s, triazole-H). ^{13}C NMR (100 MHz, $CDCl_3$) δ 26.7, 31.9, 46.9, 103.4, 107.1, 120.9, 121.9, 122.5, 122.6, 122.8, 122.9, 123.3, 123.4, 124.2, 124.3, 125.83, 126.0, 126.5, 126.6, 126.74, 126.79, 126.81, 126.85, 126.87, 127.23, 127.26, 127.3, 130.0, 130.1, 131.2, 131.4, 132.6, 134.3, 134.7,139.7, 139.8, 147.3, 147.5, 147.7, 151.6, 151.7, 154.25, 154.27, 154.9, 155.0. HRMS (ESI): calculated for $C_{49}H_{38}N_9$ $[M+H]^+$ = 752.3245; found 752.3252.

7-Methyl-2,4-bis{5-[4-(9-carbazolyl)phenyl]-1*H*-1,2,3-triazol-1-yl}-7*H*-pyrrolo[2,3-*d*]pyrimidine (4i)

Yellow solid (31 mg, 9%). mp 249 °C dec. (from 2-PrOH); ^{1}H NMR (400 MHz, d_6-DMSO): δ 4.03 (3H, s, NCH_3), 7.13 (1H, d, *J* = 3.2 Hz, 5-H), 7.16-7.25 (6H, m, carbazole-H), 7.29-7.37 (6H, m, 6-H, carbazole-H), 7.46 (2H, t, *J* = 8.0 Hz,carbazole-H), 7.82 (2H, d, *J* = 7.6 Hz, ArH), 7.93 (2H, d, *J* = 7.6 Hz, ArH), 7.97-8.00 (3H, m, carbazole-H), 8.16 (2H, d, *J* = 7.6 Hz, ArH), 8.25 (2H, d, *J* = 7.6 Hz, ArH), 8.44 (1H, s, triazole-H), 8.48 (1H, s, triazole-H). ^{13}C NMR (100 MHz, d_6-DMSO): δ 32.1, 101.9, 109.7, 110.0, 110.1, 119.7, 120.6, 120.7, 120.91, 120.96, 123.2, 123.3, 126.6, 126.68, 126.7, 126.8, 127.2, 127.3, 128.9, 131.7, 135.2, 135.4, 137.0, 138.2, 138.5, 140.1, 140.3, 146.4, 146.8, 147.85, 154.42. HRMS (ESI): calculated for $C_{47}H_{31}N_{11}Na$ $[M+Na]^+$, 772.2656; found: 772.2655

Acknowledgements

The research was supported by the Research Council of Lithuania (grant No. MIP-027/2013).

Notes and references

1 (*a*) M. T. Bernius, M. Inbasekaran, J. O'Brien abd W. S. Wu, *Adv. Mater.* 2000, **12**, 1737; (*b*) P. K. H. Ho, J. S. Kim, J. H. Burroughes, H. Becker, S. F. Y. Li, T. M. Brown, F. Cacialli and R. H. Friend, *Nature,* 2000, **404**, 481; (*c*) M. Gross, D. C. Muller, H. G. Nothofer, U. Scherf, D. Neher, C. Brauchle and K. Meerholz, *Nature,* 2000, **405**, 661; (*d*) A. P. Kulkarni, C. J. Tonzola, A. Babel and S. A. Jenekhe, *Chem. Mater.,* 2004, **16**, 4556; (*e*) G. Hughes, M. R. Bryce, *J. Mater. Chem.,* 2005, **1**,

94 (*f*) W. Y. Wong, G. J. Zhou, X. M.Yu, H. S. Kwok and Z. Lin, *Adv. Funct. Mater.,* 2007, **17**, 315; (g) Y. Tao, Q. Wang, C. Yang, Q. Wang, Z. Zhang, T. Zou, J. Qin and D. A. Ma, *Angew. Chem. Int. Ed.,* 2008, **47**, 8104-8107.

2 (*a*) S. Achelle and C. Baudequin, *In Targets in Heterocyclic Systems* (Eds.: O. A. Attanasi, D. Spinelli). Royal Society of Chemistry: London, 2013, **17**, 1; (*b*) S. Achelle and N. Ple, *Curr. Org. Synth*. 2012, **9**, 163; (*c*) S. J. Su, C. Cai and J. Kido, *Chem. Mater*., 2011, **23**, 274; (*d*) C. Hadad, S. Achelle, I. Lopez-Solera, J. C. Garcia-Martinez and J. Rodriguez-Lopez, *Dyes Pigm*. 2013, **97**, 230; (*e*) S. S. Mati, S. Chall, S. Konar, S. Rakchit, S. C. Bhattacharya, *Sensors and Actuators B*, 2014, **201**, 204; (*f*) J. Weng, Q. Mei, Q. Ling, Q. Fan, W. Huang, *Tetrahedron*, 2012, **68**, 3129.

3 For recent review on pyrimidine rings in conjugated materials, see: S. Achelle and N. Ple. *Curr. Org. Synth*. 2012, **9**, 163; For examples, see: (*a*) S. Achelle, A. Barsella, C. Baudequin, B. Caro and F. Robin-Le Guen, *J. Org. Chem.*, 2012, **77**, 4087; (*b*) J. Weng, Q. Mei, Q. Ling, Q. Fan and W. Huang, *Tetrahedron*, 2012, **68**, 3129; (*c*) I. Malik, Z. Ahmed, S. Reimann, I. Ali, A. Villinger and P. Langer, *Eur. J. Org. Chem.*, 2011, 2088; (*d*) C. Hadad, S. Achelle, J. C. Garcia-Martinez and J. Rodriguez-Lopez, *J. Org. Chem.*, 2011, **76**, 3837; (*e*) A.-S. Cornec, C. Baudequin, C. Fiol-Petit, N. Ple, G. Dupas and Y. Ramondenc, *Eur. J. Org. Chem.*, 2013, 1908; (*f*) C. Denneval, O. Moldovan, C. Baudequin, S. Achelle, P. Baldeck, N. Ple, M. Darabantu and Y. Ramondenc, *Eur. J. Org. Chem*., 2013, 5591; (*g*) D. Chen, C. Zhong, X. Dong, Z. Liu and J. Qin, *J. Mater. Chem.*, 2012, **10**, 4343; (*h*) L. Skardziute, J. Dodonova, A. Voitechovicius, J. Jovaisaite, R. Komskis, A. Voitechoviciute, J. Bucevicius, K. Kazlauskas, S. Jursenas and S. Tumkevicius, *Dyes Pigm*., 2015, **118**, 118.

4 (*a*) H. Uoyama, K. Goushi, K. Shizu, H. Nomura, C. Adachi, *Nature,* 2012, **492**, 234; (*b*) C. Adachi, *Jpn. J. Appl. Phys.,* 2014, **53**, 60101; (*c*) Y. Tao, K. Yuan, T. Chen, P. Xu, H. Li, R. Chen, C. Zheng, L. Zhang and W. Huang, *Adv. Mater.*, 2014, **26**, 7931.

5 (*a*) A. P. de Silva, T. S. Moody, G. D. Wright, Analyst, 2009, **134**, 2385; (*b*) V. D. Suryawanshi, A. H. Gore, P. R. Dongare, P. V. Anbhule, S. R. Patil and G. B. Kolekar, *Spectrochim. Acta, Part A*, 2013, **114**, 681; (*c*) Q. Meng, D. H. Kim, X. Bai, L. Bi, N. J. Turro and J. Ju, *J. Org. Chem*., 2006, **71**, 3248; (*d*) D. A. Berry, K.-Y. Jung, D. S. Wise, A. D. Sercel, W. H. Pearson, H. Mackie, J. B. Randolph and R. J. Somers, *Tetrahedron Lett.,* 2004, **45**, 2457.

6 V. V. Rostovtsev, L. G. Green, V. V. Fokin and K. B. Sharpless, *Angew. Chem. Int. Ed.* 2002, **41**, 2596.

7 C. W. Tornøe, C. Christensen and M. Meldal, *J. Org. Chem.,* 2002, **67** (9), 3057.

8 (*a*) V. D. Bock, H. Hiemstra and J. H. Maarseveen, *Eur. J. Org. Chem.*, 2006, 51; b) M. Meldal and C. W. Tornøe, *Chem. Rev.*, 2008, **108** (8), 2952.

9 (*a*) J. Gierlich, G. A. Burley, P. M. E. Gramlich, D. M. Hammond and T. J. Carell, *Org. Lett*., 2006, **8**, 3639; (*b*) R. Franke, C. Dol and J. Eichler, *Tetrahedron Lett.*, 2005, **46**, 4479. (*c*) H. Jang, A. Farman, J. M. Holub and K. J. Kirshenbaum, *Org. Lett.*, 2005, **7**, 1951; (*d*) J. M. Holub, H. Jang and K. Kirshenbaum, *Org. Biomol. Chem.*, 2006, **4**, 1497; (*e*) F. Amblard, J. H. Cho and R. F. Schinazi, *Chem. Rev.*, 2009, **109**, 4207; (*f*) A. Kovalovs, I. Novosjolova, E. Bizdena, I. Bizane, L. Skardziute, K. Kazlauskas, S. Jursenas, and M. Turks, *Tetrahedron Lett.*, 2013, **54**, 850; (*g*) I. Novosjolova, E. Bizdena and M. Turks, *Tetrahedron Lett*, 2013, **54**, 6557; (*h*) C. Dyrager, K. Börjesson, P. Dinér, A. Elf, B. L. Albinsson, M. Wilhelmsson and M. Grøtli, *Eur. J. Org. Chem.*, 2009, 1515.

10 J. E. Moses and A. D. Moorhouse, *Chem. Soc. Rev.*, 2007, **36**, 1249.

11 For recent review see Y. H. Lau, P. J. Rutledge, M. Watkinson and M. H. Todd, *Chem. Soc. Rev.*, 2011, **40**, 2848; For examples see (*a*) M. Collot, A. Lasoroski, A. I. Zamaleeva, A. Feltz, A. Vuilleumier and J. M. Mallet, *Tetrahedron Lett.*, 2013, **69**, 10482; (*b*) H. Singh, J. Sindhu and J. M. Khurana, *Sensor Actuat. B-Chem.*, 2014, **192**, 536; (*c*) L. Cao, R. Jiang, Y. Zhu, X. Wang, Y. Li and Y. Li, *Eur. J. Org. Chem.*, 2014, 2687.

12 (*a*) H. Zhang, L. Zhou, S. J. Coats, T. R. McBrayer, P. M. Tharnish, L. Bondada, M. Detorio, S. Amichai, M. D. Johns, T. Whitaker and R. F. Schinazi, *Bioorg. Med. Chem. Lett.*, 2011, **21**, 6788; (b) P. Chittepu, V. R. Sirivolu and F. Seela, *Bioorg. Med. Chem.*, 2008, **16**, 8427.

13 (*a*) S. S. Bag and R. *J.* Kundu, *Org. Chem.,* 2011, **76**, 3348; (*b*) D. Schweinfurth, K. I. Hardcastle and U. H. F. Bunz, *Chem. Commun.,* 2008, 2203; (*c*) J. Shi, L. Liu, J. He. X. Meng and Q. Guo, *Chem. Lett.,* 2007, **36**, 1142; (*d*) P. D. Jarowski, Y.-L. Wu, B. Schweizer and F. Diederich, *Org. Lett.*, 2008, **10**, 3347; (*e*) D. J. V. C. van Stennis, O. R. P. David, G. P. F. van Srijdonck, J. H. van Maarseveen, J. N. Reek, *Chem. Commun*., 2005, 4332; (*f*) M. Juricek, P. H. J. Kouwer and A. E. Rowan, *Chem. Commun.,* 2011, **47**, 874; (*g*) P. D. Zoon, I. H. M. van Stokkum, M. Parent, O. Mongin, M. Blanchard-Desce and A. M. Brouwer, *Phys. Chem. Chem. Phys.,* 2010, **12**, 2706; (*h*) D. Urankar, A. Pevec, I. Turel and J. Kosmrlj, *Cryst. Growth Des.,* 2010, **10**, 4920; (*i*) M. Parent, O. Mongin, K. Kamada, C. Katan and M. Blanchard-Desce, *Chem. Commun.,* 2005, 2029.

14 (*a*) S. Tumkevicius, J. Dodonova, K. Kazlauskas, V. Masevicius, L. Skardziute and S. Jursenas, *Tetrahedron Lett.,* 2010, **51**, 3902; (*b*) J. Dodonova, L. Skardziute, K. Kazlauskas, S. Jursenas, S. Tumkevicius, *Tetrahedron,* 2012, **68**, 329; (*c*) L. Skardziute, K. Kazlauskas, J. Dodonova, J. Bucevicius, S. Tumkevicius and S. Jursenas, *Tetrahedron*, 2013, **69**, 9566

15 (*a*) M. E. Di Francesco, S. Avolio, M. Pompei, S. Pesci, E. Monteagudo, V. Pucci, C. Giuliano, F. Fiore, R. Michael and V. Summa, *Bioorg. Med. Chem.,* 2012, **20**, 4801; (*b*) C. P. Lawson, A. Dierckx, F.-A. Miannay, E. Wellner, L. M. Wilhelmsson and M. Grotli, *Org. Biomol. Chem*., 2014, **12**, 5158; (*c*) S. A. Ingale and F. Seela, *Tetrahedron*, 2014, **70**, 380.

16 (*a*) A. S. Cornec, C. Baudequin, C. Fiol-Petit, N. Plé, G. Dupas and Y. Ramondenc, *Eur. J. Org. Chem.,* 2013, 1908; (*b*) L. I. Nilsson, A. Ertan, D. Weigelt and J. M. J. Nolsoe, J. *Heterocyclic Chem*., 2010, **47**, 887; (*c*) C. Denneval, O. Moldovan, C. Baudequin, S. Achelle, P. Baldeck, N. Plé, M. Darabantu and Y. Ramondenc, *Eur. J. Org. Chem.*, 2013, 5591

17 M. K. Lakshman, M. K. Singh, D. Parrish, R. Balachandran and B. W. Day, *J. Org. Chem.*, 2010, **75**, 2461.

18 (*a*) E. G. Paronikyan and A. S. Noravyan, *Chem. Heterocycl. Comp.*, 1995, **31** (5), 621; (*b*) C. G. Dave and R. D. Shah, *J. Heterocycl. Chem.*, 1998, **35**, 1295; (*c*) C. G. Dave and R. D. Shah, *Molecules*, 2002, **7**, 554; (*d*) N. D. Desai, Synth. Commun., 2006, **36**, 2169.

19 C. Shao, X. Wang, Q. Zhang; S. Luo, J. Zhao and Y. Hu, *J. Org. Chem.*, 2011, **76**, 6832.

20 P. M. Chandrika, T. Yakaiah, G. Gayatri, K. P. Kumar, P. Narsaiah, U. S. N. Murthy and A. R. Ram Rao, *Eur. J. Med. Chem.*, 2010, **45**, 78.

21 D. Cantillo; M. Avalos, R. Babiano, P. Cintas, J. L. Jimenez and J. C. Palacios, *Org. Biomol. Chem.*, 2011, **9**, 2952.

22 (*a*) G. Alonso, M. T. Garcia-Lopez, R. Madroner and M. J. Rico, *Heterocycl. Chem.*, 1970, **7**, 1269; (*b*) A. Bolje, D. Urankar and J. Kosmrlj, *Eur. J. Org. Chem.*, 2014, 8167.

23 Gaussian 09, Revision **D.01**, M. J. Frisch, G. W. Trucks, H. B. Schlegel, G. E. Scuseria, M. A. Robb, J. R. Cheeseman, [illegible]

Scalmani, V. Barone, B. Mennucci, G. A. Petersson, H. Nakatsuji, M. Caricato, X. Li, H. P. Hratchian, A. F. Izmaylov, J. Bloino, G. Zheng, J. L. Sonnenberg, M. Hada, M. Ehara, K. Toyota, R. Fukuda, J. Hasegawa, M. Ishida, T. Nakajima, Y. Honda, O. Kitao, H. Nakai, T. Vreven, J. A. Montgomery, Jr., J. E. Peralta, F. Ogliaro, M. Bearpark, J. J. Heyd, E. Brothers, K. N. Kudin, V. N. Staroverov, R. Kobayashi, J. Normand, K. Raghavachari, A. Rendell, J. C. Burant, S. S. Iyengar, J. Tomasi, M. Cossi, N. Rega, J. M. Millam, M. Klene, J. E. Knox, J. B. Cross, V. Bakken, C. Adamo, J. Jaramillo, R. Gomperts, R. E. Stratmann, O. Yazyev, A. J. Austin, R. Cammi, C. Pomelli, J. W. Ochterski, R. L. Martin, K. Morokuma, V. G. Zakrzewski, G. A. Voth, P. Salvador, J. J. Dannenberg, S. Dapprich, A. D. Daniels, Ö. Farkas, J. B. Foresman, J. V. Ortiz, J. Cioslowski, and D. J. Fox, Gaussian, Inc., Wallingford CT, 2009.

24 P. I. Djurovich, E. I. Mayo, S. R. Forrest and M. E. Thompson, *Org. Electron.,* 2009, **10**, 515.

25 F. Sella and H. Steker, *Liebigs. Ann. Chem.*, 1984, 1719.

26 J. Simokaitiene, S. Grigalevicius, J. V. Grazulevicius, R. Rutkaite, K. Kazlauskas, S. Jursenas, V. Jankauskas and J. Sidaravicius, *J. Optoelectron. Adv. Mater.*, 2006, **8** (*2*), 876.

27 Z. R. Grabowski and K. Rotkiewicz, *Chem. Rev.*, 2003, **103**, 3899.

28 H. Xie, L. Zeng, S. Zeng, X. Lu, G. Zhang, X. Zhao, N. Cheng, Z. Tu, Z. Li, H. Xu, L. Yang, X. Zhang, M. Huang, J. Zhao and W. Hu, *Eur. J. Med. Chem.,* 2012, **52**, 205.